

STABILITY AND NUMERICAL DISPERSION ANALYSIS OF FINITE-DIFFERENCE METHOD FOR THE DIFFUSIVE-VISCOUS WAVE EQUATION

HAIXIA ZHAO, JINGHUAI GAO*, AND ZHANGXIN CHEN

Abstract. The diffusive-viscous wave equation plays an important role in seismic exploration and it can be used to explain the frequency-dependent reflections observed both in laboratory and field data. The numerical solution to this type of wave equation is needed in practical applications because it is difficult to obtain the analytical solution in complex media. Finite-difference method (FDM) is the most common used in numerical modeling, yet the numerical dispersion relation and stability condition remain to be solved for the diffusive-viscous wave equation in FDM. In this paper, we perform an analysis for the numerical dispersion and Von Neumann stability criteria of the diffusive-viscous wave equation for second order FD scheme. New results are compared with the results of acoustic case. Analysis reveals that the numerical dispersion is inversely proportional to the number of grid points per wavelength for both cases of diffusive-viscous waves and acoustic waves, but the numerical dispersion of the diffusive-viscous waves is smaller than that of acoustic waves with the same time and spatial steps due to its more restrictive stability condition, and it requires a smaller time step for the diffusive-viscous wave equation than acoustic case.

Key words. Stability, dispersion analysis, finite-difference method, diffusive-viscous wave equation, acoustic waves

1. Introduction

The diffusive-viscous wave equation was proposed recently in the field of oil and gas exploration. The low-frequency seismic anomalies related to hydrocarbon reservoirs have lately attracted wide attention [25, 7, 17, 8]. Even though the relationship between the frequency-dependent reflections and fluid saturation in a reservoir can be quite complex, but there is a general connection between the character of porous medium saturation and seismic response. Goloshubin and Bakulin observed phase shifts and energy redistribution between different frequencies when comparing cases of water-saturated and gas-saturated rocks [14, 12]. Korneev et al. observed that reflections from a fluid-saturated layer have increased amplitude and delayed traveltimes at low frequencies when compared with reflections from a dry layer in both laboratory and field data [17]. Those observed results cannot be explained using Biot theory [12, 3, 4, 5, 21, 10, 2], nor by the reflection properties of an elastic layer [17], or the squirt flow and patchy saturation models [20]. Korneev et al. proposed a diffusive-viscous model to explain the frequency-dependent phenomena in fluid-saturated porous reservoirs [17]. Therefore, the diffusive-viscous theory is important in seismic exploration, for example, it can be used for detecting and monitoring hydrocarbon reservoirs [15], and it is also essential to simulate the propagation of the diffusive-viscous waves in practical applications.

Seismic numerical modeling is a valuable tool for seismic interpretation and an essential part of seismic inversion algorithms. Another important application of seismic modeling is the evaluation and design of seismic surveys [6]. There are

Received by the editors February 2, 2014 and, in revised form, March 20, 2014.

2000 *Mathematics Subject Classification.* 35R35, 49J40, 60G40.

This research was supported by National Natural Science Foundation of China (40730424) and National Science & Technology Major Project (2011ZX05023-005).

many approaches to seismic modeling. The finite-difference method(FDM) is the most straightforward numerical approach in seismic modeling, and it is also becoming increasingly more important in the seismic industry and structural modeling due to its relative accuracy and computational efficiency [22]. Some of the most common FDMs used in seismic modeling are explicit, and thus conditionally stable. Generally in seismology, explicit methods are preferred over implicit ones because they need less computation at each time step and have the same order of accuracy. This has been noted for FDM [6, 11]. However, the size of the time step is bounded by a stability criterion which is an important factor affecting the accuracy of the results. Additionally, a numerical dispersion (grid dispersion) related to grid spacing has a detrimental effect on accuracy of FD scheme. It occurs because the actual velocity of high-frequency waves in the grid is different from the true velocity and it can occur even when the physical problem is not dispersive [9]. The error introduced by numerical dispersion is dependent on the grid spacing and the size of the time step. There are many studies in literature regarding the numerical dispersion and stability analysis for acoustic wave propagation [1, 19]. However, the numerical dispersion analysis and stability condition is rarely seen despite its significance in seismic exploration for the diffusive-viscous wave propagation.

Our aims in this paper are to estimate the Von Neumann stability criteria and derive the numerical dispersion relation for the finite-difference method for the diffusive-viscous wave equation proposed by Korneev [17]. We will show that there are some differences of stability condition and dispersion relation between the diffusive-viscous wave equation and acoustic wave equation, and the dispersion of diffusive-viscous waves is smaller than that of acoustic waves with the same time and spatial steps because of its more restrictive stability condition, and it requires a smaller time step for the diffusive-viscous wave equation than acoustic case.

2. The diffusive-viscous theory

In this section, we will first introduce the diffusive-viscous wave equation, then give the propagating wavenumber and attenuation coefficient of the diffusive-viscous waves prepared for the following section.

2.1. The diffusive-viscous wave equation. The diffusive-viscous theory is proposed by Korneev [17, 13], which is used to explain the relationship between the frequency dependence of reflections and the fluid saturation in a reservoir. The diffusive-viscous wave equation in a 1-D medium is mathematically described as follows:

$$(1) \quad \frac{\partial^2 u}{\partial t^2} + \gamma \frac{\partial u}{\partial t} - \eta \frac{\partial^3 u}{\partial x^2 \partial t} - v^2 \frac{\partial^2 u}{\partial x^2} = 0$$

for $(x, t) \in (-\infty, \infty) \times [0, \infty)$, where u is the wave field; $\gamma \geq 0$, $\eta \geq 0$ are diffusive and viscous attenuation parameters, respectively, which are the functions of the porosity and the permeability of reservoir rocks and the viscosity and the density of the fluid; v is the wave propagation velocity in a non-dispersive medium. The second term in (1) characterizes a diffusional dispersive force, whereas the third term describes the viscosity. t is the time and x is the space variables. Equation (1) is extended to two dimensional case (2-D) as [15]

$$(2) \quad \frac{\partial^2 u}{\partial t^2} + \gamma \frac{\partial u}{\partial t} - \eta \left(\frac{\partial^3 u}{\partial x^2 \partial t} + \frac{\partial^3 u}{\partial z^2 \partial t} \right) - v^2 \left(\frac{\partial^2 u}{\partial x^2} + \frac{\partial^2 u}{\partial z^2} \right) = 0$$

The definitions of the variables are the same as (1), and $(x, z) \in (-\infty, \infty) \times (-\infty, \infty)$ are the Cartesian coordinates.

2.2. The propagating wavenumber and attenuation coefficient of the diffusive-viscous wave. To derive a harmonic plane wave solution of (2), we take a form as given below

$$(3) \quad u(x, z, t) = e^{i(\omega t - \tilde{k}_x x - \tilde{k}_z z)}$$

with angular frequency ω and the wave numbers \tilde{k}_x, \tilde{k}_z along x and z directions, respectively. And note that $\tilde{k}_x^2 + \tilde{k}_z^2 = \tilde{k}^2$, \tilde{k} is the complex wavenumber, and it can be in the form as

$$(4) \quad \tilde{k} = k + i\alpha$$

where, k is the propagation wavenumber, and α is the attenuation coefficient of diffusive-viscous waves, and $i = \sqrt{-1}$.

Substituting (3) into (2), we get

$$(5) \quad -\omega^2 + \gamma(i\omega) + \eta\tilde{k}^2(i\omega) + v^2\tilde{k}^2 = 0$$

From (5), we have

$$(6) \quad \tilde{k}^2 = \frac{\omega^2 - i\gamma\omega}{v^2 + i\eta\omega} = \frac{(v^2\omega^2 - \gamma\eta\omega^2) - i(\eta\omega^3 + \gamma\omega v^2)}{v^4 + \eta^2\omega^2} = \tilde{K}_R + i\tilde{K}_I$$

where, $\tilde{K}_R = \frac{v^2\omega^2 - \gamma\eta\omega^2}{v^4 + \eta^2\omega^2}$, $\tilde{K}_I = -\frac{\eta\omega^3 + \gamma\omega v^2}{v^4 + \eta^2\omega^2}$ are the real and imaginary parts of \tilde{k}^2 .

According to (4), we can also obtain

$$(7) \quad \tilde{k}^2 = k^2 + i2k\alpha - \alpha^2$$

Then, the propagation wavenumber k and attenuation coefficient α can be obtained by combing (6) and (7) as

$$(8) \quad k = \pm \sqrt{\frac{\tilde{K}_R + \sqrt{(\tilde{K}_R^2 + \tilde{K}_I^2)}}{2}}, \alpha = \frac{\tilde{K}_I}{2k} = \pm \frac{\tilde{K}_I}{2\sqrt{\frac{\tilde{K}_R + \sqrt{(\tilde{K}_R^2 + \tilde{K}_I^2)}}{2}}}$$

The sign of the attenuation coefficient α in (8) is determined by the attenuation property of diffusive-viscous waves, and both k and α not only depend on parameters of the medium, but also vary significantly with frequency. These two variables will be used in the following section.

3. The Von Neumann stability criteria of diffusive-viscous wave equation

Finite-difference computations require determinations of spatial and temporal sampling criteria. As pointed out by Kelly and Marfurt [16], spatial sampling is generally chosen to avoid numerical dispersion in solutions. Then, the temporal sampling is chosen to avoid numerical instability. The stability analysis for FD solutions of partial differential equations is handled using a method originally developed by Von Neumann [24]. In this section, we will give the stability criteria for FD solution of diffusive-viscous wave equation following this method, and compare the results of this equation with acoustic case.

We denote the exact solution of (2) by $U(x, z, t)$. If we assume the grid to be uniform, let $h > 0$ be the spatial sampling step and let $(x_j, z_m) = (jh, mh)$, $j = 0, 1, 2, \dots, N_x$, $m = 0, 1, 2, \dots, N_z$, be the nodal points and $t_n = n\Delta t$, $n = 1, 2, \dots, N_t$, be the time points with time step of Δt , and N_x, N_z are the total numbers of samples in x, z directions, respectively; N_t is the total number of temporal samples. The values of the solution at each (x_j, z_m, t_n) are then given by $U(x_j, z_m, t_n) = U_{j,m}^n$. And we denote the derivatives of the solution with respect to x, z , at each (x_j, z_m, t_n)

by $U'_x(x_j, z_m, t_n) = U'_{x_j, m}{}^n$, $U'_z(x_j, z_m, t_n) = U'_{z_j, m}{}^n$, respectively, and similarly for higher derivatives; for example, $U''_{xx}(x_j, z_m, t_n) = U''_{xx_j, m}{}^n$, $U''_{zz}(x_j, z_m, t_n) = U''_{zz_j, m}{}^n$, etc. Then we use a central difference formula to discretize $U''_{xx}(x, z, t)$, $U''_{zz}(x, z, t)$, $U''_{tt}(x, z, t)$ by expanding $U(x, z, t)$ in a Taylor series at $j + 1, j - 1, m + 1, m - 1$, and $n + 1, n - 1$, respectively, given by

$$(9) \quad \begin{aligned} U''_{xx}(x_j, z_m, t_n) &\approx \frac{U_{j+1, m}^n - 2U_{j, m}^n + U_{j-1, m}^n}{h^2}, \\ U''_{zz}(x_j, z_m, t_n) &\approx \frac{U_{j, m+1}^n - 2U_{j, m}^n + U_{j, m-1}^n}{h^2}, \\ U''_{tt}(x_j, z_m, t_n) &\approx \frac{U_{j, m}^{n+1} - 2U_{j, m}^n + U_{j, m}^{n-1}}{(\Delta t)^2} \end{aligned}$$

And we use a backward difference formula to discretize $U'_t(x, z, t)$, by expanding $U(x, z, t)$ in a Taylor series at $n - 1$, given by

$$(10) \quad U'_t(x_j, z_m, t_n) \approx \frac{U_{j, m}^n - U_{j, m}^{n-1}}{\Delta t}$$

We now define a numerical approximation $u_{j, m}^n$ to the exact solution $U_{j, m}^n$. Using the discretization (9) and (10), the approximate solution $u_{j, m}^n$ associated with the equation (2) in rectangular coordinates satisfies

$$(11) \quad \begin{aligned} u_{j, m}^{n+1} &= [2 - 4a - \gamma(\Delta t) - 4b]u_{j, m}^n \\ &\quad - [1 - \gamma(\Delta t) - 4a]u_{j, m}^{n-1} - a(u_{j+1, m}^{n-1} + u_{j-1, m}^{n-1} + u_{j, m+1}^{n-1} + u_{j, m-1}^{n-1}) \\ &\quad + (a + b)(u_{j+1, m}^n + u_{j-1, m}^n + u_{j, m+1}^n + u_{j, m-1}^n) \end{aligned}$$

where, $a = \frac{\eta\Delta t}{h^2}$, $b = \frac{v^2(\Delta t)^2}{h^2}$.

The actual error of the wavefield at (x_j, z_m, t_n) is defined as

$$(12) \quad \varepsilon_{j, m}^n = U_{j, m}^n - u_{j, m}^n$$

Substituting (12) into the FD scheme (11), we obtain

$$(13) \quad \begin{aligned} &U_{j, m}^{n+1} - \{[2 - 4a - \gamma(\Delta t) - 4b]U_{j, m}^n - [1 - \gamma(\Delta t) - 4a]U_{j, m}^{n-1} \\ &\quad - a(U_{j+1, m}^{n-1} + U_{j-1, m}^{n-1} + U_{j, m+1}^{n-1} + U_{j, m-1}^{n-1}) \\ &\quad + (a + b)(U_{j+1, m}^n + U_{j-1, m}^n + U_{j, m+1}^n + U_{j, m-1}^n)\} \\ &= \varepsilon_{j, m}^{n+1} - \{[2 - 4a - \gamma(\Delta t) - 4b]\varepsilon_{j, m}^n - [1 - \gamma(\Delta t) - 4a]\varepsilon_{j, m}^{n-1} \\ &\quad - a(\varepsilon_{j+1, m}^{n-1} + \varepsilon_{j-1, m}^{n-1} + \varepsilon_{j, m+1}^{n-1} + \varepsilon_{j, m-1}^{n-1}) \\ &\quad + (a + b)(\varepsilon_{j+1, m}^n + \varepsilon_{j-1, m}^n + \varepsilon_{j, m+1}^n + \varepsilon_{j, m-1}^n)\} \end{aligned}$$

Note that the expression of (13) on the left side is the truncation error, and the expression of (13) on the right side is the propagation equation for actual error. We say that a method is numerically stable if the actual error $\varepsilon_{j, m}^n$ is bounded as $n \rightarrow \infty$. For simplicity, we will only consider the propagation of the error and assume the truncation error is zero. For example, in the FD scheme, this assumption implies the error propagates according to

$$(14) \quad \begin{aligned} &\varepsilon_{j, m}^{n+1} - \{[2 - 4a - \gamma(\Delta t) - 4b]\varepsilon_{j, m}^n - [1 - \gamma(\Delta t) - 4a]\varepsilon_{j, m}^{n-1} \\ &\quad - a(\varepsilon_{j+1, m}^{n-1} + \varepsilon_{j-1, m}^{n-1} + \varepsilon_{j, m+1}^{n-1} + \varepsilon_{j, m-1}^{n-1}) \\ &\quad + (a + b)(\varepsilon_{j+1, m}^n + \varepsilon_{j-1, m}^n + \varepsilon_{j, m+1}^n + \varepsilon_{j, m-1}^n)\} = 0 \end{aligned}$$

In order to analyze the stability of (14), we will decompose the error in terms of Fourier modes or waves with certain wavelengths. This approach is known as the Von Neumann method of investigating stability [23].

An error of wave type can be written as

$$(15) \quad \begin{aligned} \varepsilon_{j,m}^n &= \varepsilon^n e^{i(\tilde{k}_x x_j + \tilde{k}_z z_m)} \\ &= \varepsilon^n e^{i(jh\tilde{k}_x + mh\tilde{k}_z)} \end{aligned}$$

where ε^n is the amplitude of the wave at time n .

We substitute (15) into (14), obtaining

$$(16) \quad \begin{aligned} \varepsilon^{n+1} &= \varepsilon^n \{2 - \gamma(\Delta t) - 4(a+b)[\sin^2(\frac{\tilde{k}_x h}{2}) + \sin^2(\frac{\tilde{k}_z h}{2})]\} \\ &\quad - \varepsilon^{n-1} \{1 - \gamma(\Delta t) - 4a[\sin^2(\frac{\tilde{k}_x h}{2}) + \sin^2(\frac{\tilde{k}_z h}{2})]\} \end{aligned}$$

Equation (16) has been analyzed for stability providing a sufficient condition for stability by considering the ratio of the error Fourier amplitudes as a function of time steps [23]. That is, we consider this ratio as $R = \frac{\varepsilon^{n+1}}{\varepsilon^n} = \frac{\varepsilon^n}{\varepsilon^{n-1}}$ to be the ratio of successive iterations. Therefore, we can insure stability by requiring that $|R| \leq 1$.

We consider the stability in terms of R by dividing equation (16) by ε^{n-1} to obtain

$$(17) \quad \begin{aligned} R^2 - R\{2 - \gamma(\Delta t) - 4(a+b)[\sin^2(\frac{\tilde{k}_x h}{2}) + \sin^2(\frac{\tilde{k}_z h}{2})]\} \\ + \{1 - \gamma(\Delta t) - 4a[\sin^2(\frac{\tilde{k}_x h}{2}) + \sin^2(\frac{\tilde{k}_z h}{2})]\} = 0 \end{aligned}$$

Denoting by

$$(18) \quad \begin{aligned} A &= 2 - \gamma(\Delta t) - 4(a+b)[\sin^2(\frac{\tilde{k}_x h}{2}) + \sin^2(\frac{\tilde{k}_z h}{2})], \\ B &= 1 - \gamma(\Delta t) - 4a[\sin^2(\frac{\tilde{k}_x h}{2}) + \sin^2(\frac{\tilde{k}_z h}{2})] \end{aligned}$$

Then, (17) can be rewritten as

$$(19) \quad R^2 - AR + B = 0$$

such that

$$(20) \quad R = \frac{A \pm \sqrt{(A^2 - 4B)}}{2}$$

And the stability condition for FD scheme is turning to solve the problem as

$$(21) \quad \left| \frac{A \pm \sqrt{(A^2 - 4B)}}{2} \right| \leq 1$$

After some complex mathematical operations, A and B in (21) have to satisfy

$$(22) \quad \begin{aligned} -2 &\leq A \leq 2, \\ 0 &\leq B \leq \frac{A^2}{4}, \\ B &\geq -1 - A, \\ B &\geq -1 + A \end{aligned}$$

For the sake of clarity, Figure 1 shows the variation of B with respect to A , the pink lined area 1 and area 2 illustrate the intersection area of A and B satisfying the inequalities (22).

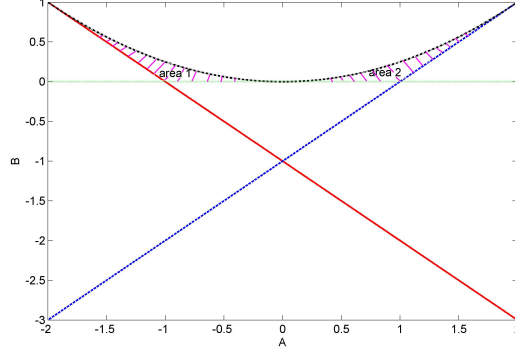


FIGURE 1. Variation of B with respect to A under the condition of the inequalities (22)

From inequality (22) and Figure 1, we can clearly see that the range of values of A and B is

$$(23) \quad \begin{aligned} -2 \leq A \leq 2, \\ 0 \leq B \leq 1 \end{aligned}$$

Returning (18), we also find that

$$(24) \quad \begin{aligned} 2 - \gamma(\Delta t) - 8(a + b) \leq A \leq 2 - \gamma(\Delta t), \\ 1 - \gamma(\Delta t) - 8a \leq B \leq 1 - \gamma(\Delta t) \end{aligned}$$

Inequalities (23) and (24) show that

$$(25) \quad \begin{aligned} \gamma \geq 0, \Delta t \geq 0, \\ \Delta t \leq \frac{\sqrt{6} h}{4 v}, \\ \Delta t \leq \frac{h^2}{\gamma h^2 + 8\eta} \end{aligned}$$

The inequalities (25) imply that the time step Δt must satisfy (26) in order to ensure the stability of second order FD scheme for the diffusive-viscous wave equation (2).

$$(26) \quad 0 \leq \Delta t \leq \min\left(\frac{\sqrt{6} h}{4 v}, \frac{h^2}{\gamma h^2 + 8\eta}\right)$$

Where, "min" represents the minimum value of quantities.

The diffusive-viscous wave equation is reduced to acoustic wave equation when $\gamma = \eta = 0$. In this case, the Von Neumann stability of acoustic wave equation can be obtained from (21) with $A = 2 - 4b[\sin^2(\frac{k_x h}{2}) + \sin^2(\frac{k_z h}{2})]$ and $B = 1$ [19]. That is

$$(27) \quad \Delta t \leq \frac{1}{\sqrt{2}} \frac{h}{v}$$

From (26) and (27), we can clearly find that the stability criteria of diffusive-viscous wave equation for second order FD scheme is not only determined by the spatial step and velocity of the medium, but also depends on the diffusive and viscous attenuation parameter γ and η . However, it is only determined by the spatial step and velocity of the medium for acoustic case. Additionally, it requires

a smaller time step for diffusive-viscous wave equation than acoustic case with the same parameters of the media and spatial steps.

4. Numerical dispersion of diffusive-viscous wave equation

In this section, we will first derive the numerical dispersion relation for the diffusive-viscous wave equation, and then we will perform the dispersion analysis numerically for the FD scheme (11) with comparison of acoustic case.

4.1. Derivations of numerical dispersion relation. The dispersive nature of the waveforms can be examined by considering phase velocity as a function of frequency or, equivalently, as a function of G (the number of grid points per wavelength). The absence of dispersion would, of course, be characterized by phase velocity that does not vary with frequency [1]. Expression for phase velocity based on plane wave propagation of diffusive-viscous waves for the second-order FD scheme is derived in the following.

To derive the dispersion relation, the harmonic plane wave in the form of (3) is used again, and we substitute (3) into (11) and obtain

$$\begin{aligned}
& e^{i\omega(n+1)\Delta t} e^{-i(jh\bar{k} \cos \theta + mh\bar{k} \sin \theta)} \\
&= [2 - 4a - \gamma(\Delta t) - 4b] e^{i\omega n \Delta t} e^{-i(jh\bar{k} \cos \theta + mh\bar{k} \sin \theta)} \\
& - [1 - \gamma(\Delta t) - 4a] e^{i\omega(n-1)\Delta t} e^{-i(jh\bar{k} \cos \theta + mh\bar{k} \sin \theta)} \\
(28) \quad & - a \{ e^{i\omega(n-1)\Delta t} [e^{-i[(j+1)h\bar{k} \cos \theta + mh\bar{k} \sin \theta]} + e^{-i[(j-1)h\bar{k} \cos \theta + mh\bar{k} \sin \theta]} \\
& + e^{-i[jh\bar{k} \cos \theta + (m+1)h\bar{k} \sin \theta]} + e^{-i[jh\bar{k} \cos \theta + (m-1)h\bar{k} \sin \theta]}] \} \\
& + (a+b) \{ e^{i\omega n \Delta t} [e^{-i[(j+1)h\bar{k} \cos \theta + mh\bar{k} \sin \theta]} + e^{-i[(j-1)h\bar{k} \cos \theta + mh\bar{k} \sin \theta]} \\
& + e^{-i[jh\bar{k} \cos \theta + (m+1)h\bar{k} \sin \theta]} + e^{-i[jh\bar{k} \cos \theta + (m-1)h\bar{k} \sin \theta]}] \}
\end{aligned}$$

where θ is the angle between the direction of propagation and the x -axis.

After some complex algebra operations, (28) finally becomes

$$\begin{aligned}
(29) \quad -4 \sin^2 \frac{\omega \Delta t}{2} &= (e^{-i\omega \Delta t} - 1) [\gamma(\Delta t) + 4a (\sin^2 \frac{\tilde{k}h \cos \theta}{2} + \sin^2 \frac{\tilde{k}h \sin \theta}{2})] \\
& - 4b (\sin^2 \frac{\tilde{k}h \cos \theta}{2} + \sin^2 \frac{\tilde{k}h \sin \theta}{2})
\end{aligned}$$

Denoting by $p = \frac{v(\Delta t)}{h}$ and $G = \frac{\lambda}{h}$ which is the number of grid points per wavelength, then

$$(30) \quad \frac{kh}{2} = \frac{2\pi h}{\lambda} \frac{h}{2} = \frac{\pi}{G}$$

And the normalized phase velocity $\frac{C_p}{v}$ is given as

$$(31) \quad \frac{C_p}{v} = \frac{\omega}{k} \frac{1}{v} = \frac{\omega \Delta t}{k p h} = \frac{\omega \lambda \Delta t}{2\pi p h} = \frac{\omega \Delta t}{2} \frac{G}{\pi p}$$

Where, λ is the wavelength, and $C_p = \frac{\omega}{k}$ is the phase velocity of the diffusive-viscous wave equation.

Thus, the normalized phase velocity $\frac{C_p}{v}$ varies with G, p and ω , but the angle frequency ω is controlled by formula (29), which implies that we cannot obtain the explicit expression of relationship between ω and θ . From the function point of

view in formula (29), the angle frequency ω is the function of θ , determined by the following implicit function $W(\omega, \theta)$ as

$$(32) \quad W(\omega, \theta) = (e^{-i\omega\Delta t} - 1) \left[\gamma(\Delta t) + 4a \left(\sin^2 \frac{\tilde{k}h \cos \theta}{2} + \sin^2 \frac{\tilde{k}h \sin \theta}{2} \right) \right. \\ \left. - 4b \left(\sin^2 \frac{\tilde{k}h \cos \theta}{2} + \sin^2 \frac{\tilde{k}h \sin \theta}{2} \right) + 4 \sin^2 \frac{\omega\Delta t}{2} \right]$$

Substituting the expression of complex wavenumber of (4) and formula (30) into (32), one gets

$$(33) \quad W(\omega, \theta) = (e^{-i\omega\Delta t} - 1) \left\{ \gamma(\Delta t) + 4a \left[\sin^2 \left(\frac{\pi h \cos \theta}{G} + \frac{i\alpha h \cos \theta}{2} \right) \right. \right. \\ \left. \left. + \sin^2 \left(\frac{\pi h \sin \theta}{G} + \frac{i\alpha h \sin \theta}{2} \right) \right] \right\} - 4b \left[\sin^2 \left(\frac{\pi h \cos \theta}{G} + \frac{i\alpha h \cos \theta}{2} \right) \right. \\ \left. + \sin^2 \left(\frac{\pi h \sin \theta}{G} + \frac{i\alpha h \sin \theta}{2} \right) \right] + 4 \sin^2 \frac{\omega\Delta t}{2}$$

where, α is the attenuation coefficient of diffusive-viscous waves, defined in (8).

According to the implicit function theorem [18], there exists a function $\omega = f(\theta)$ satisfying $W[f(\theta), \theta] = 0$. However, it is impossible to obtain the exact expression of the function $\omega = f(\theta)$ from (29), here we resort to gain the approximate relationship between ω and θ using the least square method as

$$(34) \quad \min | W(\omega, \theta) |_{\theta=fixed\ value}^2 \Rightarrow \omega \approx f(\theta)$$

The minimization problem (34) means that we find the values of ω when the function $W(\omega, \theta)$ reach a minimum at fixed values of θ . So, we can obtain a series of values of ω when θ takes a certain range of values. From (29), (31)-(34), we can see that the normalized phase velocity $\frac{C_p}{v}$ varies with θ and G, p . Therefore, from the function point of view in formula (31), it can be rewritten as

$$(35) \quad Y_{cp}(G, \theta, p) \approx f(\theta) \frac{\Delta t}{2} \frac{G}{\pi p}$$

In formula (35) we have denoted $\frac{C_p}{v}$ by $Y_{cp}(G, \theta, p)$.

In the case of acoustic waves, the numerical dispersion relation can be easily obtained from (29) with $\gamma = \eta = 0$. That is

$$(36) \quad \sin^2 \frac{\omega\Delta t}{2} = b \left(\sin^2 \frac{k_c h \cos \theta}{2} + \sin^2 \frac{k_c h \sin \theta}{2} \right)$$

In this case, $k_c = \frac{\omega}{v}$, $\alpha = 0$. Then, the normalized phase velocity for acoustic wave equation can be obtained from (30) and (36) as

$$(37) \quad \frac{C_p^c}{v} = \frac{G}{p\pi} \arcsin \sqrt{b \left[\sin^2 \left(\frac{\pi \cos \theta}{G} \right) + \sin^2 \left(\frac{\pi \sin \theta}{G} \right) \right]}$$

Where, C_p^c is the phase velocity of acoustic wave.

From (29) and (36), we can clearly see that the dispersion relation of diffusive-viscous wave equation is much more complex than that of acoustic case, and it significantly depends on the diffusive and viscous attenuation parameters γ and η , which are determined by the properties of the media. And we can not obtain the explicit expression of phase velocity of diffusive-viscous wave equation but the explicit expression of phase velocity of acoustic wave equation can be easily obtained. Thus, there are some differences of numerical dispersion properties between diffusive-viscous waves and acoustic waves for second order FDM.

4.2. Numerical dispersion analysis. In this section, we will present the numerical dispersion curves of the diffusive-viscous waves for second order FDM by comparing those of acoustic case using the method that we presented in the previous section. And we will investigate the effects that the stability parameter p , the angle θ , the number of grid points per wavelength G and the parameters of the media have in the numerical dispersion.

Table 1 describes the parameters of the three types of media. Figure 2, Figure 4 and Figure 6 show the numerical dispersion results of second order FDM for the diffusive-viscous wave equation with comparison of those of acoustic waves (see Figure 3, Figure 5 and Figure 7) in three medium (dry sandstone, water-saturated and oil-saturated rocks) with $p = 0.496$, $p = 0.6125$ and $p = 0.406$, respectively. Therefore, from those results we can draw some conclusions as:

1) The dispersion is greatest when the wave propagates parallel to the grid ($\theta = 0$ degree);

2) The dispersion is smallest if we take a time step close to the stability condition (see Figure 4 and Figure 5), which indicates that it should be made as large as possible to minimize dispersion and the maximum value is determined by the stability limit of (26) and (27);

3) A minimum of 10 nodes per wavelength is recommended to achieve accurate results for second order FDM;

4) Angle frequency decreases with the number of grid points per wavelength for both cases of diffusive-viscous waves and acoustic waves (see Figure 2(a) - Figure 7(a));

5) The numerical dispersion of second order FD scheme is inversely proportional to the number of grid points per wavelength for both cases of diffusive-viscous waves and acoustic waves (see Figure 2(b) - Figure 7(b));

6) The numerical dispersion of second order FD scheme increases with the angle (0-45 degrees) between the direction of wave propagation and x -axis for both cases of diffusive-viscous waves and acoustic waves (see Figure 2(c) - Figure 7(c));

7) However, the numerical dispersion of diffusive-viscous waves is smaller than that of acoustic waves with the same time and spatial steps because of their different stability limits, and it requires a smaller time step for diffusive-viscous wave equation than acoustic case with the same spatial step and the same parameters of the media. We note that the results of 1)-3) are consistent with the conclusions in [1].

TABLE 1. Parameters of medium

| medium | v /(m/s) | γ /Hz | η /(m ² /s) |
|----------------------|------------|--------------|-----------------------------|
| dry sandstone | 1190 | 56 | 0.056 |
| water-saturated rock | 1470 | 90 | 0.2 |
| oil-saturated rock | 1015 | 65.4 | 0.0147 |

5. Conclusions

We present the stability condition and numerical dispersion relation of the diffusive-viscous wave equation for second order FDM, and further analyze the numerical dispersion properties by comparing the results of acoustic case. The results show that the stability limits are different for diffusive-viscous wave equation and acoustic wave equation, and it requires a smaller time step for the diffusive-viscous wave equation than acoustic case with the same parameters of the media. Moreover, we

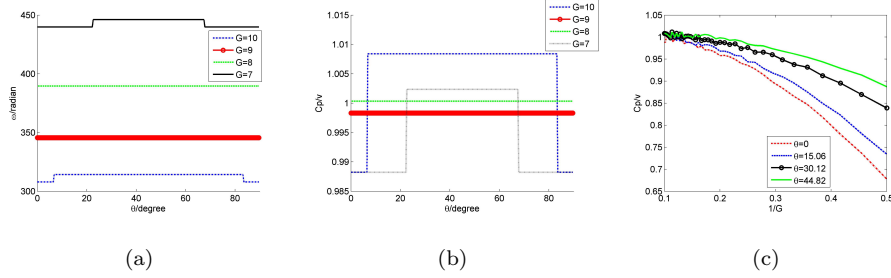


FIGURE 2. (a) Angle frequency varies with the angle θ between the direction of wave propagation and x -axis, (b) Normalized phase velocity C_p/v varies with the angle θ and (c) Normalized phase velocity of second order FDM as a function of the sampling ratio G , with angles of 0, 15.06, 30.12, and 44.82 degrees. Those results are obtained in dry sandstone medium for diffusive-viscous wave equation with $p = 0.496$. The time step is controlled by the stability condition (26).

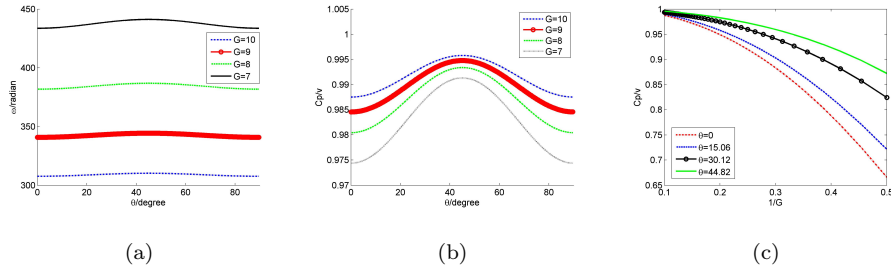


FIGURE 3. (a) Angle frequency varies with the angle θ between the direction of wave propagation and x -axis, (b) Normalized phase velocity C_p^c/v varies with the angle θ and (c) Normalized phase velocity of second order FDM as a function of the sampling ratio G , with angles of 0, 15.06, 30.12, and 44.82 degrees. Those results are obtained in dry sandstone medium for acoustic wave equation with $p = 0.496$. The time step is controlled by the stability condition (27).

obtain the same conclusions published in the literature for both cases. However, the numerical dispersion of the diffusive-viscous waves is smaller than that of acoustic waves with the same time and spatial steps due to its more restrictive stability condition. Finally, we bear in mind that more dispersion may arise from boundary conditions, irregular grids, or heterogeneities in the medium in practical applications. The results of this paper provide a better understanding of the numerical dispersion and stability properties of FDM for the diffusive-viscous wave equation.

6. Acknowledgements

The authors would like to thank all the teachers and students in Institute of Wave and Information at Xi'an Jiaotong University, and we also greatly appreciate National Science Foundation of China (40730424) and National Science & Technology Major Project (2011ZX05023-005) for their support.

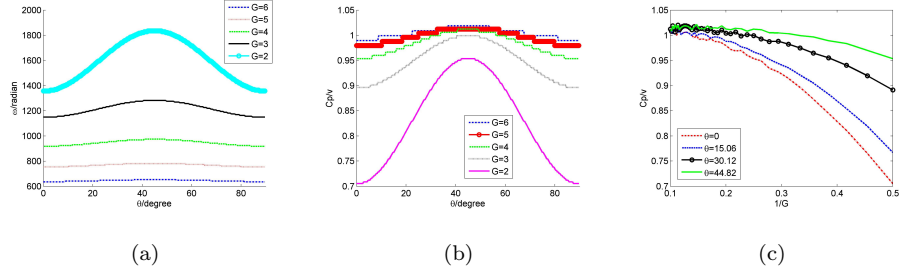


FIGURE 4. (a) Angle frequency varies with the angle θ between the direction of wave propagation and x -axis, (b) Normalized phase velocity C_p/v varies with the angle θ and (c) Normalized phase velocity of second order FDM as a function of the sampling ratio G , with angles of 0, 15.06, 30.12, and 44.82 degrees. Those results are obtained in water-saturated medium for diffusive-viscous wave equation with $p = 0.6125$. The time step is controlled by the stability condition (26).

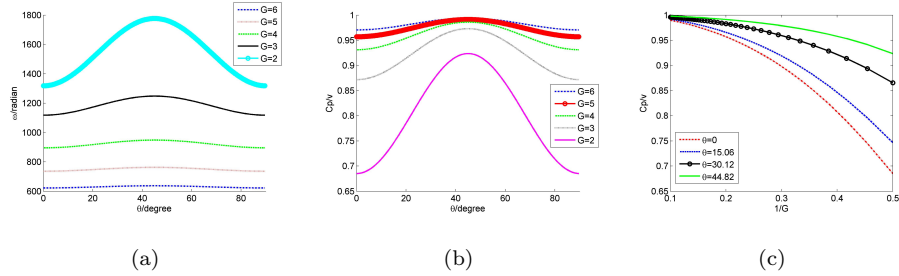


FIGURE 5. (a) Angle frequency varies with the angle θ between the direction of wave propagation and x -axis, (b) Normalized phase velocity C_p^c/v varies with the angle θ and (c) Normalized phase velocity of second order FDM as a function of the sampling ratio G , with angles of 0, 15.06, 30.12, and 44.82 degrees. Those results are obtained in water-saturated medium for acoustic wave equation with $p = 0.6125$. The time step is controlled by the stability condition (27).

References

- [1] RM Alford, KR Kelly, and D.M. Boore. Accuracy of finite-difference modeling of the acoustic wave equation. *Geophysics*, 39(1974):834C842.
- [2] B. Arntsen and J.M. Carcione. Numerical simulation of the biot slow wave in water-saturated nivelsteiner sandstone. *Geophysics*, 66(2001):890C896.
- [3] M.A. Biot. Theory of propagation of elastic waves in a fluid-saturated porous solid. i. low-frequency range. *The Journal of the Acoustical Society of America*, 28(1956),168-178.
- [4] M.A. Biot. Theory of propagation of elastic waves in a fluid-saturated porous solid. ii. higher frequency range. *The Journal of the Acoustical Society of America*, 28(1956):179C191.
- [5] MA Biot. Generalized theory of acoustic propagation in porous dissipative media. *The Journal of the Acoustical Society of America*, 34(1962):1254C1264.
- [6] J.M. Carcione, G.C. Herman, and APE Ten Kroode. Seismic modeling. *Geophysics*, 67(2002):1304C1325.

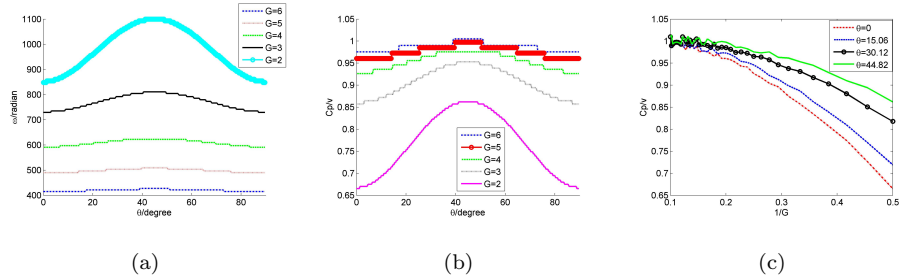


FIGURE 6. (a) Angle frequency varies with the angle θ between the direction of wave propagation and x -axis, (b) Normalized phase velocity C_p/v varies with the angle θ and (c) Normalized phase velocity of second order FDM as a function of the sampling ratio G , with angles of 0, 15.06, 30.12, and 44.82 degrees. Those results are obtained in oil-saturated medium for diffusive-viscous wave equation with $p = 0.406$. The time step is controlled by the stability condition (26).

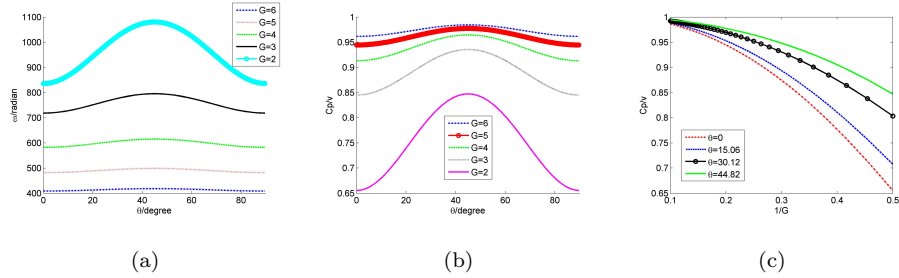


FIGURE 7. (a) Angle frequency varies with the angle θ between the direction of wave propagation and x -axis, (b) Normalized phase velocity C_p^c/v varies with the angle θ and (c) Normalized phase velocity of second order FDM as a function of the sampling ratio G , with angles of 0, 15.06, 30.12, and 44.82 degrees. Those results are obtained in oil-saturated medium for acoustic wave equation with $p = 0.406$. The time step is controlled by the stability condition (27).

- [7] J.P. Castagna, S. Sun, and R.W. Siegfried. Instantaneous spectral analysis detection of low-frequency shadows associated with hydrocarbons. *The Leading Edge*, 22(2003):120C127.
- [8] M. Chapman, E. Liu, and X.Y. Li. The influence of fluid-sensitive dispersion and attenuation on AVO analysis. *Geophysical Journal International*, 167(2006):89C105.
- [9] J.D. De Basabe and M.K. Sen. Grid dispersion and stability criteria of some common finite-element methods for acoustic and elastic wave equations. *Geophysics*, 72(2007):T81CT95.
- [10] J. Dvorkin, G. Mavko, and A. Nur. Squirt flow in fully saturated rocks. In 1993 SEG Annual Meeting, 1993.
- [11] S.H. Emerman, W. Schmidt, and RA Stephen. An implicit finite-difference formulation of the elastic wave equation. *Geophysics*, 47(1982):1521C1526.
- [12] GM Goloshubin and AV Bakulin. Seismic reflectivity of a thin porous fluid-saturated layer versus frequency. In 1998 SEG Annual Meeting, 1998.
- [13] G.M. Goloshubin and V.A. Korneev. Seismic low-frequency effects from fluid-saturated reservoir. In 2000 SEG Annual Meeting, 2000.

- [14] GM Goloshubin, AM Verkhovsky, and VV Kaurov. Laboratory experiments of seismic monitoring. In EAGE 58th Conference and Technical Exhibition, Amsterdam, The Netherlands, Geophysical Division, volume 2(1996):3C7.
- [15] Z. He, X. Xiong, and L. Bian. Numerical simulation of seismic low-frequency shadows and its application. Applied Geophysics, 5(2008):301C306.
- [16] KR Kelly. Numerical modeling of seismic wave propagation, volume 13. Soc of Exploration Geophysicists, 1990.
- [17] V.A. Korneev, G.M. Goloshubin, T.M. Daley, and D.B. Silin. Seismic low-frequency effects in monitoring fluid-saturated reservoirs. Geophysics, 69(2004):522C532.
- [18] S.G. Krantz and H.R. Parks. The implicit function theorem: history, theory, and applications. Birkh?user Boston, 2002.
- [19] L.R. Lines, R. Slawinski, and R.P. Bording. A recipe for stability analysis of finite-difference wave equation computations. Geophysics, 64(1999):967C969.
- [20] G. Mavko, T. Mukerji, and J. Dvorkin. Rock physics handbook: Tools for seismic interpretation in porous media 1998.
- [21] S. Mochizuki. Attenuation in partially saturated rocks. Journal of Geophysical Research, 87(1982):8598C8604.
- [22] P. Moczo, J.O.A. Robertsson, and L. Eisner. The finite-difference time-domain method for modeling of seismic wave propagation. Advances in Geophysics, 48(2007):421C516.
- [23] I.R. Mufti. Large-scale three-dimensional seismic models and their interpretive significance. Geophysics, 55(1990):1166C1182.
- [24] W.H. Press, B.P. Flannery, S.A. Teukolsky, and W.T. Vetterling. Numerical Recipes in FORTRAN 77: Volume 1, Volume 1 of Fortran Numerical Recipes: The Art of Scientific Computing, volume 1. Cambridge university press, 1992.
- [25] M.T. Taner, F. Koehler, and RE Sheriff. Complex seismic trace analysis. Geophysics, 44(1979):1041C1063.

National Engineering Laboratory for Offshore Oil Exploration, Institute of Wave and Information, School of Electronic and Information Engineering, Xi'an Jiaotong University, Xi'an 710049, China

E-mail: relindadb2010@gmail.com and jhgao@mail.xjtu.edu.cn

Center for Computational Geoscience, Xi'an Jiaotong University, Xi'an 710049, China. Department of Chemical and Petroleum Engineering, University of Calgary, Calgary, Alberta, T2N 1N4, Canada.

E-mail: zhachen@ucalgary.ca